JOURNAL OF THERMOPHYSICS AND HEAT TRANSFER
Vol. 20, No. 3, July–September 2006

Fluidization Behavior of Fine Powders in Reduced Gravity Conditions

Rui Shao,* Richard R. Williams,† and Ruel A. Overfelt‡
Auburn University, Auburn, Alabama 36832

Geldart's traditional powder classification of the fluidization process in Earth's gravitational acceleration is very well known. In this paper, the fluidization behaviors of spherical glass powders and aluminum-oxide powders with different mean particle sizes were studied at four gravitational-acceleration conditions: 1.8 *g*, 1.0 *g*, 0.38 *g* (Martian gravity), and 0.16 *g* (lunar gravity). The transition region between Geldart's group A and group C powders was determined at each gravitational acceleration. The observed results were compared to Qian et al.'s semitheoretical group A/C transition equation with good agreement at 1.8 *g* and 1.0 *g* and a divergence at 0.38 *g* and 0.16 *g*, and the observed results indicated a stronger dependence upon gravity.

Nomenclature

A	=	Hamaker constant
d_p	=	particle diameter
F_H	=	cohesion force
g	=	local gravitational acceleration
l	=	diameter of the asperities of a powder particle
δ	=	particle spacing
ε	=	bed void volume
ρ_p	=	particle density
ρ_f	=	fluid density

I. Introduction

GENERALLY, the fluidization process "is formed by passing a fluid, usually a gas, upwards through a bed of particles supported on a distributor."[1] Compared with the other powder processes, the fluidization process has a high mass and heat transfer efficiency and has been widely used in industry. The major applications of fluidization processes can be classified in two areas: the first includes physical processes such as drying, filtration, coating, and heat exchange; the second includes chemical processes, such as chemical reactions; coal, biomass, waste combustion; and gasification.

NASA's exploration initiative to return to the moon and land on Mars will require the ability to effectively perform critical processes outside of Earth's gravity and utilize in situ resources. These processes include, among others, the ability to make repairs to critical systems, the ability to fabricate spare parts utilizing either in situ or prestaged raw materials, the ability to process waste into usable resources, and the ability to transform in situ resources into usable products. Although most of these processes currently do not exist in extraterrestrial form, all of them potentially may need to utilize fine particulates or powders. Therefore, the knowledge and understanding of how to transport, convey, fluidize, and defluidize powders in low-gravity extraterrestrial environments underpins the successful implementation of these enabling technologies and hence the successful achievement of NASA's mission.

Received 24 February 2005; revision received 19 May 2005; accepted for publication 25 May 2005.

*Graduate Research Assistant, Materials Processing Center, 275 Wilmore Labs.

†Associate Research Professor, Materials Engineering, 259 Wilmore Labs; currently, Assistant Professor, Technology Systems, East Carolina University, 202 Slay Hall, Greenville, NC 27858; williamsric@mail.ecu.edu.

‡Professor, Materials Engineering, 282 Wilmore Labs.

The specific class of powders that were studied in this work is powder that may behave cohesively. In Earth's gravity, this is generally any powder with a particle diameter of less than 20 μm. Lunar soils have been shown to be made up of a significant mass percentage (ca. 50%) of particles less than 60 μm in diameter.[2] Although there has been no Martian soil returned to Earth for analysis, it is reasonable to expect some similarities between Martian soil and lunar soil because they are both fine-grained silty soils.[3] Additionally, powders with diameters typically greater than 20 μm are generally not considered cohesive in Earth's gravity. However, these powders may become cohesive in low gravity (even Martian or lunar gravity). As a result, current powder technologies that are considered mature and well understood here on Earth will behave much differently in an extraterrestrial environment.

Geldart[4] classified powders in the fluidization process based upon experimental observations according to the particle density and mean particle size as group C, group A, group B and group D. Table 1 lists the distinguishable differences among the four groups. In general, group A powders are aeratable and easily fluidize without bubbling, thus the maximum efficiency of mass and heat transfer can be achieved; group B powders fluidize with bubble generation occurring at the minimum fluidization velocity; group D powders, which are characterized by large particle sizes, spout with increasing flow velocity; and group C powders, called "cohesive powders," are extremely difficult to fluidize because of their large specific surface area, thus leading to interparticle forces that are much greater than that which the fluid can exert on the particles. Normally the group C powders lift up as a plug at lower flow velocity, and when the flow velocity increases, channeling occurs. As a consequence, the mass and heat transfer rates in group C powders are much poorer than those in group A or B powders. Geldart's fluidization process map is illustrated in Fig. 1. Geldart developed this diagram for fluidization processes occurring with air at 1 atm and 1.0 *g*. As illustrated in Fig. 1, group C powders are generally small-particle-diameter (typically <20 μm) powders.

Fine micrometer, submicrometer, or even nanometer powders are preferred for modern pharmaceutical and chemical-engineering processes because fine powders have unique characteristics such as high surface-to-volume ratios and low activation energies. Moreover, the fluidization process is a very powerful technique and also can be used to study the mechanism behind the cohesive phenomenon of fine powders. Therefore, studying the fluidization behavior of group C powders and developing techniques to improve the fluidization behavior of fine powders are topics of current interest.

Presently, the methods used to improve fluidization behaviors of group C powders can be divided into three categories: 1) redesign or reconfiguration of the fluidization bed, such as adding magnetic fields,[5] vibration,[6,7] rotation,[8] and acoustic energy[9]; 2) manipulation of particle or fluid properties, including particle sizes[10,11] and coatings[12]; and 3) the gravitational-force effect.[8,13] Although

Table 1 Geldart's classification of powder[1]

Properties	Group C	Group A	Group B	Group D
Major characteristic	Cohesive, difficult to fluidize	Ideal for fluidization; a range of nonbubbling fluidization exists	Bubbling at min. fluidization velocity	Coarse solids
Bed expansion	Low, because of channeling	High	Moderate	Low
Bubble properties	No bubbles; channels and cracks	Splitting and recoalescence predominate; maximum size exists; large wake	No limit on size	No limit on size
Slug properties	Solid slugs	Axisymmetric	Axisymmetric, asymmetric	Horizontal voids, solid slugs, wall slugs
Spouting	No	No	Shallow beds only	Yes

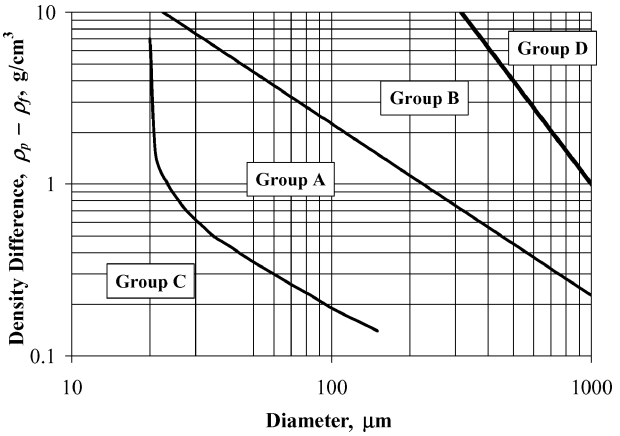

Fig. 1 Geldart's fluidization process map.[4]

gravitational force plays an important role in the fluidization process, there is not a large amount of research focusing on gravity because most experiments and fluidization processes are carried out in Earth's gravity and there are limited methods to change gravitational acceleration.

Molerus[13] first developed the semiempirical equation for the transition between group A and group C powders (group A/C transition) by considering the force balance between the cohesion forces and the hydrodynamic forces exerted from the gas on the particles. Group C powders satisfied the following equation:

$$10(\rho_p - \rho_f)d_p^3 g \Big/ F_H \leq 10^{-2} \tag{1}$$

where ρ_p and ρ_f are powder and fluid density respectively, F_H is the cohesion force, d_p is particle diameter, and g is the local gravitational acceleration. This criterion shows that when the density difference between particle and fluid is constant, the group A/C transition will move into the 1.0 g group A regime with decreasing gravitational acceleration; that is, the group C powder regime extends to larger particle sizes.

Qian et al.[8] considered the critical difference between group C and group A powders to be that group A powders can be fluidized individually, whereas group C powders fluidized as agglomerates. They considered Van der Waals force to be the only force contributing to the cohesion force. Based upon these assumptions, a semitheoretical equation that maps the transition between group C and group A behavior was given as

$$\left(\pi g d_p^3 \Big/ 6\right)(\rho_p - \rho_f)(\varepsilon^{-4.8} - \varepsilon) = Al/24\delta^2 \tag{2}$$

where l is the diameter of the asperities of a powder particle, δ is the distance between two particles, A is the Hamaker constant, and ε is void volume or porosity of the fluidized bed. Using Eq. (2), Qian et al. pointed out that the group A/C transition would be affected by the gravitational acceleration. With the gravitational acceleration increasing, the transition curve between group A and group C powders would shift to the left on Fig. 1 to smaller particle diameters. Qian et al. verified this hypothesis by conducting an experiment where they artificially increased gravity using centrifugal force by rotating the bed. They found that some powders that behaved as group C in Earth's gravity behaved as group A powders at high rotational speeds, which were as high as 278 g. To our knowledge, Eq. (2) has not been previously validated at gravity values less than 1.0 g. However, it is likely that the trend is correct; as gravity is reduced, the group A/C transition curve of Fig. 1 shifts to the right. In other words, powders that behave as group A in Earth's gravity may behave as group C in lower-gravity environments. This fact underscores the importance of understanding the behavior of fine powders in reduced-gravity environments to achieving the goal of reliably processing materials in extraterrestrial environments. Processes and technologies that currently use powders that are not considered cohesive (because of the particle size) in 1.0 g may behave very differently in low-gravity environments.

In the present work, the fluidization behaviors of aluminum-oxide and glass powers of different particle sizes were studied at 1.8-g, 1.0-g, 0.38-g, and 0.16-g acceleration conditions. Except for the 1.0-g case, 1.8-g, 0.38-g, and 0.16-g conditions were obtained in parabolic flight on NASA's Reduced Gravity Platform (http://jsc-aircraft-ops.jsc.nasa.gov/Reduced_Gravity/). These results provide required information for exploiting the fluidization process for applications in extraterrestrial environments, such as on the moon or Mars. The present research verifies the shift of transition-boundary curve between group A and group C powders at various gravitational accelerations less than 1.0 g.

II. Experiment

A. Experiment Setup

A fluidized bed platform was specifically designed for the parabolic flight onboard NASA's KC-135 Reduced Gravity Platform. Four transparent acrylic cylinders with diameters of 7.62 cm and heights of 76 cm constituted a multibed assembly and were mounted side by side on a vibration table. Three strips of electrically grounded copper tape were tightly pressed on the inner surface of each acrylic cylinder to minimize electrostatic buildup. A porous metal plate with a characteristic pore diameter of 2 μm was used as the gas distributor. A digital video camera located in front of the fluidization beds was used to optically characterize the experiment results. Gas temperature, gas volumetric flow rate, and the pressure drop across the beds were also recorded. A gas-distribution system allowed for the fluidization of a single bed at a given time. To maintain the required safety assurance during the flight, the entire assembly (except for the gas cylinders) was mounted into one fixed frame. A schematic diagram and photographs of the experiment setup are shown in Figs. 2 and 3, respectively.

The criterion for powder selection was based on the elimination of the influence of the specific characteristics of the powders other than particle size and density. In addition, the particle diameter must span the transition regime of group A/C powders. Commercially available aluminum oxide (Extec Corp., Enfield, CT) and glass powders (Potters Industries, Valley Forge, PA) were used in this experiment. The properties of the powders are listed in Table 2. Dry glass powders, A1–A4, each with different mean particle sizes, were loaded into one set of the multibed assembly. Dry aluminum-oxide powders, B1–B4, were similarly placed into a second set of the multibed assembly. These assemblies could be easily exchanged to allow for the

Table 2 Properties of powders used in the present work

	Powders classification							
Parameter	A1	A2	A3	A4	B1	B2	B3	B4
Type	Glass	Glass	Glass	Glass	Aluminum oxide	Aluminum oxide	Aluminum oxide	Aluminum oxide
Shape	Spherical	Spherical	Spherical	Spherical	Irregular	Irregular	Irregular	Irregular
Density, g/cm^3	2.5	2.5	2.5	2.5	3.77	3.77	3.77	3.77
Mean particle diameter (μm)	11	20	35	71	12	13	18	45
Geldart's classification at 1.0 g	Group C	Group C	Group A	Group A	Group C	Group C	Group C	Group A

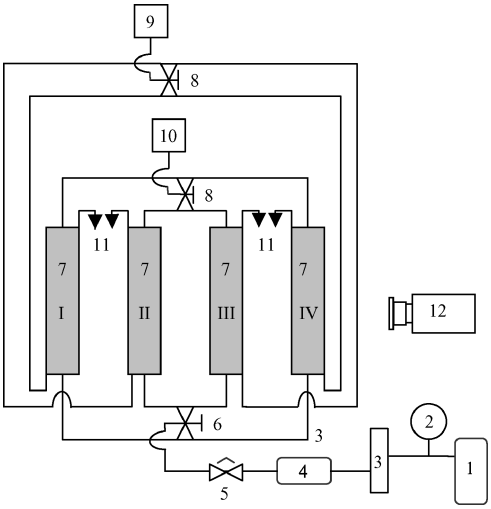

Fig. 2 Schematic of the fluidization bed: 1, gas cylinder; 2, pressure gauge; 3, mass flow meter; 4, 5-μm filter; 5, flow control valve; 6, chamber selection valve; 7, I, II, III, IV fluidization chambers; 8, pressure transducer selection valve; 9, inlet pressure transducer; 10, exit pressure transducer; 11, gas exit; and 12, digital video camera.

study of either material. Each bed was filled to an unexpanded height of approximately 10 cm. The top of each cylindrical chamber was capped by a desiccant material to prevent moisture intrusion into the beds and the desiccant was removed prior to running the experiment.

B. Experimental Procedures

The operation of an experiment onboard NASA's KC-135 Reduced Gravity Platform is challenging because of the high pace of each successive parabola and short duration of the desired low-gravity environment. Each parabolic cycle was on the order of 1.5 min with the low-gravity portion typically lasting 25 to 30 s. The procedure outlined here was utilized to effectively operate the experiment in this environment.

First, the desired bed within the multibed assembly was selected by aligning the chamber selection valve, the pressure transducers, and the camera to the required positions. Next, to maintain as near as possible a constant initial powder-packing state, a 5-s vibration of the bed was initiated just prior to entering the desired gravity segment of the parabola (i.e., 1.8 g, 0.38 g, or 0.16 g) and initiating the gas flow into the fluidized bed. The vibrator was operated at a frequency of 60 Hz and at an amplitude of 2.5 g. Vibration was secured and flow was initiated upon reaching the desired gravity level using the flow control valve. Flow was continuously increased until the bed fluidized, lifted, cracked, spouted, or channeled. The gas flow was secured upon exiting the reduced gravity portion of the parabola and the cycle was repeated for the next bed or gravity level. The flow rate, pressure drop, temperature, video data, and an audio log were collected and recorded throughout the entire parabola set. The flow rate, pressure drop, and temperature data were not directly used in this experiment; however, no anomalies were noted within these data. Each powder was tested at least twice at each gravity level.

Both dry nitrogen gas and dry helium gas were used as the fluidization gas in the experiment. However, because of inclement weather, the cycles of parabolic flight were reduced and, as a consequence, the data from helium gas fluidization was not sufficient to analyze. Therefore, only the experimental results of nitrogen have been reported and discussed herein.

a)

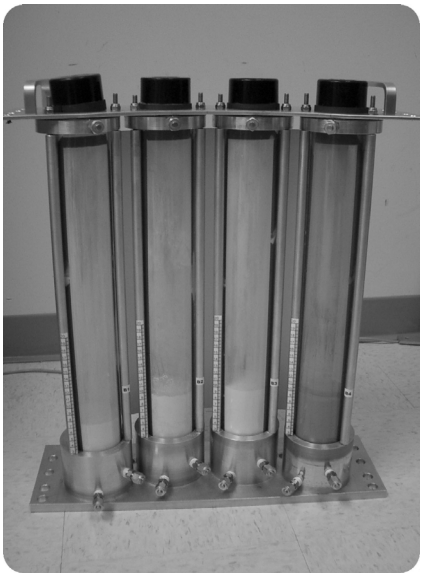

b)

Fig. 3 Fluidized bed platform: a) the front view of the fluidization bed setup and b) multibed assembly.

III. Results and Discussion

A. Gravitational Acceleration Effect on Glass Powders

The major characteristics of the fluidization process were observed in this experiment, such as fluidizing, bubbling, channeling, and spouting. The observed results are listed in Table 3 in terms

Table 3 Fluidization behaviors of glass powder at various gravitational acceleration

Gravitational acceleration, g	Geldart powder classification			
	A1, 11 μm	A2, 20 μm	A3, 35 μm	A4, 71 μm
1.8	C	A	A	B
1.0	C	A−	A	B
0.38	C	C	A−	B
0.16	C	C	C	A

Table 4 Fluidization behaviors of aluminum-oxide powders at various gravitational acceleration

Gravitational acceleration, g	Geldart powder classification			
	B1, 12 μm	B2, 13 μm	B3, 18 μm	B4, 45 μm
1.8	C	A−	A	A
1.0	C	C	A−	A
0.38	C	C	C	A−
0.16	C	C	C	C

of Geldart's classification scheme. A powder classified as group C, group A, or group B clearly exhibited the fluidization characteristics of the respective group. The classification of A− was assigned to powders that appeared to be very close to the transition between group A and group C. These powders initially acted cohesively but fluidized as they broke up at increasing gas flow rates.

From these observations, the effect of gravitational acceleration on the group A/C transition is clearly evident. The position of the group A/C transition curve shifted into the 1.0-g group A regime with decreasing gravitational acceleration. In other words, powders characterized by large-diameter particles behaved cohesively as the gravitational acceleration was decreased. As a result, some powders that fluidize at 1.0 g, such as powder A2, became cohesive with reduced gravitational acceleration. In addition, for the same powder at different gravitational accelerations, different fluidization behaviors were observed. For example, powder A1 was classified as group C at all four gravitational accelerations; however, the fluidization behavior of powder A1 varied with the different gravitational accelerations. At 1.8 g, a plug lifted and then dropped easily, and the bed greatly expanded with channeling; however, at 0.16 g, the plug rose without breaking until reaching the top of fluidization chamber. These different fluidization behaviors are caused by the cohesive force becoming more dominant within the system as the gravitational acceleration diminishes.

B. Gravitational Acceleration Effect on Aluminum-Oxide Powders

The same scheme as used with the glass powders was used to classify the fluidization behavior of the aluminum-oxide powders. The observed fluidization behaviors of the aluminum-oxide powders are shown in Table 4.

From Table 4, it is again clearly evident that the position of the group A/C transition shifted into the 1.0-g group A regime with decreasing gravitational acceleration. Powders such as B3 and B4 that easily fluidized at a gravitational acceleration of 1.0 g behaved cohesively at reduced gravitational accelerations. At 0.16 g, all aluminum-oxide powders within this experiment were observed to behave cohesively.

C. Comparison to Other Powder Classifications in the Fluidization Process

Using the empirical observations listed in Tables 3 and 4, the powder diameter representing the transition between group A and group C behavior was determined for each material at each level of gravitation acceleration. This was done applying the following two assumptions: 1) at a given gravitational acceleration, the transition diameter was assumed to occur at the mean diameter located between observed group C behavior and observed group A behavior, and 2) if a powder was assigned a fluidization behavior of A−, then the transition was assumed to occur at that powder diameter. For example, for glass powders at 1.8 g, powder A1 exhibited group C behavior, whereas powder A2 exhibited group A behavior; therefore, the transition was assumed to occur at the mean diameter between these two powders, or at a powder diameter of 15.5 μm. An uncertainty of ±33% of the difference between the transition diameter and the powder diameters reported in Table 2 on either side of the chosen transition diameter was placed upon the transition diameter.

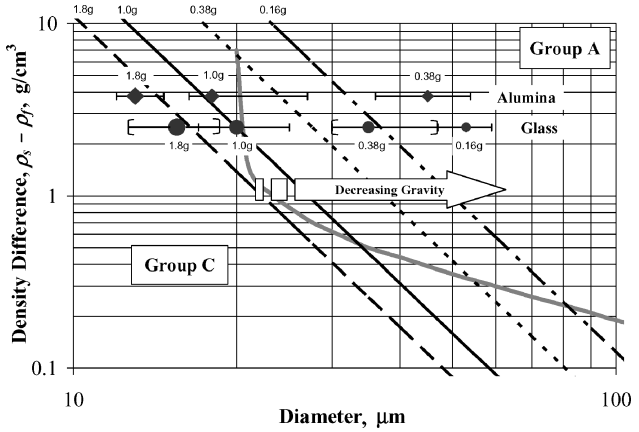

Fig. 4 Transition curve between group A/C powders from Geldart[1] (curved line), Qian et al.[8] (straight lines), and the present experiment results (data points with error bars to indicate the transition range).

Qian et al.[8] derived the semitheoretical Eq. (2) to describe the effect of gravitational acceleration on transition between group A and group C powders. Qian et al. assumed that $A = 10^{-19}$ J, $l = 0.2$ μm, and $\delta = 4$ Å. The voidage for group C particles is different for different materials and Qian et al. assumed an upper limit of $\varepsilon = 0.53$ and a lower limit of $\varepsilon = 0.4$. For this work it was not possible to directly measure the voidage at the point of fluidization; therefore a constant value of $\varepsilon = 0.44$, which provided good agreement at 1.0 g, was utilized. Using these assumptions, the density difference as a function of diameter for each magnitude of gravitational acceleration was calculated. The relationships between density difference and particle size at each gravitational acceleration (1.8 g, 1.0 g, 0.38 g, and 0.16 g) are shown in Fig. 4. In addition, Geldart's empirical 1.0-g classification curve of the group A/C transition and the empirical results from our experiment are also plotted in Fig. 4. As shown in Fig. 4, the position of the group A/C transition curve with respect to gravity as measured by this experiment was in good agreement with Qian et al. at 1.8 g and 1.0 g but was in poor agreement at 0.38 g and 0.16 g. In fact, it appears that a stronger dependence upon gravity was observed in this experiment than predicted by the model of Qian et al.

The dependence upon gravity was further investigated by assuming all the variables of Eq. (2), except d_p, ρ_p, ρ_f, and g, are constant, resulting in

$$d_p^3(\rho_p - \rho_f) = C/g^n \tag{3}$$

where $C = Al/4\pi\delta^2(\varepsilon^{-4.8} - \varepsilon)$. Applying these assumptions, $C = 1.95 \times 10^{-10}$ N and $n = 1$ and for Qian et al's model.[8] Figure 5 shows a plot of $d_p^3(\rho_p - \rho_f)$ vs g for the observed values of this experiment and as predicted by Eq. (3), applying the previous assumptions. The constants C and n for a best-fit regression on the observed data were determined to be 12.38×10^{-10} N and 1.72 respectively. The difference between the values of C in Qian et al.'s model and the current experimental result was most likely from a combination of experimental uncertainty and the assumption that all powders were assumed to have the same constant value of $\varepsilon = 0.44$. The difference between the values of n was most likely from a combination of experimental uncertainty, the constant voidage assumption, and a true increase in the dependence upon gravitational acceleration of the observed data when compared to Qian et al.'s model. The increased dependence upon gravitational acceleration was further supported by the fact that none of the aluminum-oxide powders fluidized at 0.16 g. This means that the group A/C transition curve fell above a particle diameter of 45 μm with a high degree of certainty, whereas Qian et al.'s model predicts a transition particle diameter of 39 μm using a value of ε as high as 0.50. According to

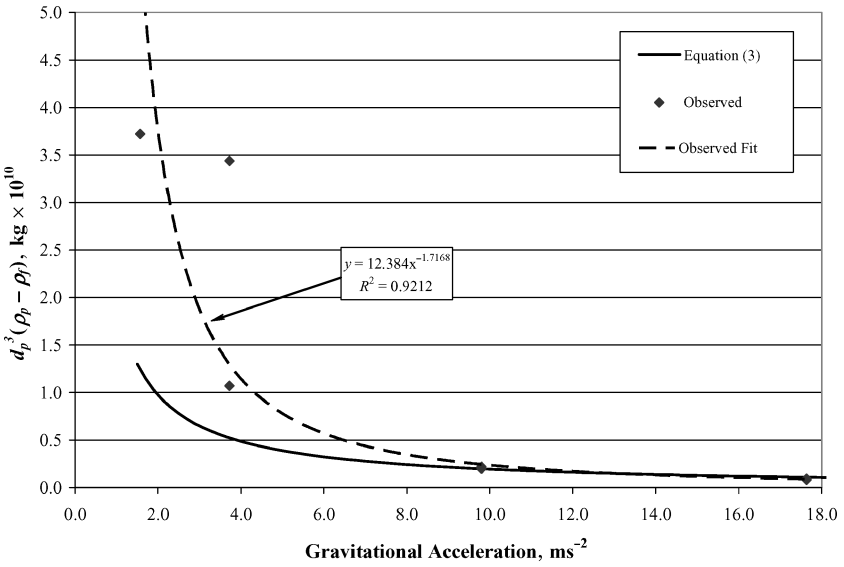

Fig. 5 Gravitational acceleration dependence of the group A/C transition for the observed data and Qian et al.'s[8] model.

Qian et al., hard materials tend to have voidages that fall closer to a value of $\varepsilon = 0.40$, whereas soft materials have voidages closer to a value of $\varepsilon = 0.53$. Given the fact that aluminum oxide is a hard material, one would expect the voidage to be closer to a value of $\varepsilon = 0.40$; however, in a reduced-gravity condition, it may be that the voidage is higher than typically reported at 1.0 *g* because the reduced gravity may not pack the particles as tightly. However, there was no measurable bed expansion of the nonfluidizing settled beds, even in zero-*g* conditions, indicating that other forces within the bed were sufficient to prevent significant particle rearrangement when gravity was reduced within the system. Nonetheless, the observations of the present experiment indicated that the group A/C transition curve depended more strongly upon gravity than predicted by the model of Qian et al. Whether this is due to a dependence of the voidage ε upon gravitational acceleration or some other mechanism can not be determined by the present work.

Qian et al.'s[8] group A/C transition curves were from a theoretical analysis in which the only cohesive force is the Van der Waals force. As is well known, the actual cohesive effects may include electrostatic, surface tension, magnetic, and mechanical binding effects, among others. Accounting for these additional cohesive effects may provide better agreement between the present observations and Qian et al.'s theoretical model. Conversely, it can be argued that there is reasonable agreement between the data of the present work and Qian et al.'s theoretical model given the somewhat subjective nature of this experiment coupled with the fairly simple assumptions of Qian et al.'s model. This uncertainly might be resolved if suitable particle-size powders were chosen to more precisely map the group A/C transition region within the range of 30–60 μm.

IV. Conclusion

Powders that readily fluidize and are classified as Geldart group A powders at a gravitational acceleration of 1.0 *g* become cohesive and may not fluidize at reduced gravitational acceleration, such as those found on the moon or Mars.

Acknowledgments

The authors graciously thank NASA for their support via Contract No. NCC8-240 and for the support of the crew of the NASA Reduced Gravity Research Program Office. We also acknowledge and thank Stevie Best, Michael Crumpler, David Hodo, Robert Langley, John Marcell, Bruce Strom, and Matthew Zorn for their valued contributions to this work.

References

[1]Geldart, D., *Gas Fluidization Technology*, Wiley, New York, 1986, Chap. 3.

[2]Heiken, G., Vaniman, D., and French, B. (eds.), *Lunar Sourcebook*, Cambridge University Press, Cambridge, England, U.K., 1991, Chap. 7.

[3]Chua, K. M., and Johnson, S. W., "Martian and Lunar Cold Region Soil Mechanics Considerations," *Journal of Aerospace Engineering*, Vol. 11, No. 4, Oct. 1998, pp. 138–147.

[4]Geldart, D., "Types of Gas Fluidization," *Powder Technology*, Vol. 7, No. 5, May 1973, pp. 285–292.

[5]Zhu, Q., and Li, H., "Study on Magnetic Fluidization of Group C Powders," *Powder Technology*, Vol. 86, No. 2, Feb. 1996, pp. 179–185.

[6]Thomas, B., Mason, M. O., and Squires, A. M., "Some Behaviors of Shallow Vibrated Beds Across a Wide Range in Particle Size and Their Implications for Powder Classification," *Powder Technology*, Vol. 111, No. 1–2, 21 Aug. 2000, pp. 34–49.

[7]Noda, K., Mawatari, Y., and Uchida, S., "Flow Patterns of Particles in a Vibrated Fluidized Bed Under Atmospheric or Reduced Pressure," *Powder Technology*, Vol. 99, No. 1, Sept. 1998, pp. 11–14.

[8]Qian, G., Bágye, I., Burdick, I. W., Pfeffer, R., and Shaw, H., "Gas–Solid Fluidization in a Centrifugal Field,"*Particle Technology and Fluidization*, Vol. 47, No. 5, May 2001, pp. 1022–1034.

[9]Zhu, C., Liu, G., Yu, Q., Pfeffer, R., Dave, R. N., and Nam, C. H., "Sound Assisted Fluidization of Nanoparticle Agglomerates," *Powder Technology*, Vol. 141, No. 1–2, March 2004, pp. 119–123.

[10]Wang, Z., and Li, H., "A New Criterion for Prejudging the Fluidization Behavior of Powders," *Powder Technology,* Vol. 84, No. 2, Aug. 1995, pp. 191–195.

[11]Wang, Z., Kwauk, M., and Li, H., "Fluidization of Fine Particles," *Chemical Engineering Science*, Vol. 53, No. 3, Feb. 1998, pp. 377–395.

[12]Karches, M., and Rohr, P. R. V., "Microwave Plasma Characteristics of a Circulating Fluidized Bed Plasma Reactor for Coating Powders," *Surface and Coating Technology*, Vol. 142–144, July 2001, pp. 28–33.

[13]Molerus, O., "Interpretation of Geldart's Type A, B, C and D Powders by Taking into Account Interparticle Cohesion Forces," *Powder Technology*, Vol. 33, No. 1, 1982, pp. 81–87.